ARCHIVES
of
FOUNDRY ENGINEERING

ISSN (1897-3310)
Volume 16
Issue 1/2016

131 – 137

23/1

Published quarterly as the organ of the Foundry Commission of the Polish Academy of Sciences

Tin-Copper-Lead Alloy Produced by Horizontal Centrifugal Casting

S.E.Vahdat
Department of Engineering, Ayatollah Amoli Branch,
Islamic Azad University, Amol, Iran
*Corresponding author. E-mail address: seyed_ebrahim_vahdat@yahoo.com

Received 13.03.2015; accepted in revised form 17.07.2015

Abstract

Horizontal centrifugal casting is an effective method for the production of hollow metal with good mechanical properties, low defect, cast to size and relatively cheap. The ability of a metal to satisfy the above requirements highly depends on its microstructure. In this study, the relationship between microstructural parameters such as grain size and the amount of phases with bulk hardness of SnCu4Pb3 is concerned in three areas of the product. Consequently, to achieve the desired hardness of the product in a particular area, the interaction of two factors of the microstructure including, grain size and particles amount of the hard intermetallic compositions (Cu_6Sn_5) should be noted.

Keywords: Functionally graded materials, Phase diagram;

1. Introduction

As the increasing demands particularly in the shipbuilding and railways industry,study of engineering properties in order to save energy resources and raw materials causes pouring products of desired properties and cast-to-size. Competition of metallic materials with composite materials for desirable engineering properties and finally dispose of the pressure vessels due to segregation and internal stresses caused by traditional casting and in the other hand, progress in automobile and aircraft causes foundry industry can no longer rely on traditional ideas of non-scientific arguments to continue. Hence the need to engineering infrastructure and pay attention to science quickly became so wide as without any doubt can be stated that in the near future the casting will have correlation with the logical and mathematical concepts.

In centrifugal casting, the centrifugal force is used in addition to the gravity force to fill the mold. In this method, the outer surface of product is formed by the internal surface of the mold but the inner surface (free surface) of product is formed due to affected by centrifugal force on it and after solidification it is removed from the mold as a hollow cylindrical shape. Casting temperature of the alloy is higher than the melting temperature of the alloy for in situ centrifugal casting process, and therefore heavier elements will be closer to the (mold) wall and thus secondary phases will be distributed and formed during solidification of the alloy [1-6].

The density of tin, lead and copper are 7.26, 11.30 and 8.96 g/cm3[7]. In centrifugal casting using centrifugal force, heavy/light phase goes towards the outside/free surface of product, and thus the distribution of heavy/light phase is provided functionally graded. For this purpose the density difference between the secondary and the melt phase/phases must be remarkable. For this reason, these types of products with functionally graded properties in alloys with wide solidification range are produced more easily.

Phase diagram of a ternary Sn-Cu-Pb in Figure 1 (a) shows that the alloy contains 92.7 wt% (92.56 mol%) tin, 3.1 wt% (5.41 mol%) lead and 3.8 wt% (2.03 mol%) copper along with impurities such as zinc, aluminum, silver, iron, bismuth and antimony with wide solidification range. It is predicted in the microstructure of the mentioned alloy, in the tin matrix, there are

about 10 wt% hard phase of Cu_6Sn_5 in Figure 1 (b), and less than 3 wt% solid solution containing 4 mol% (2.39 wt%) tin and 96 mol% (97.61 wt %) lead in Figure 1 (c).
Because of differences in the density of the constituent elements of tin-copper-lead alloy, a chemical composition near the mold is different from a chemical composition near the free surface of product, so it leads to changes in the microstructure and the hardness in different areas (Figure. 2 (a)). The purpose is to determine the relationship between microstructure and hardness of the investigated alloy in the horizontal centrifugal casting process.

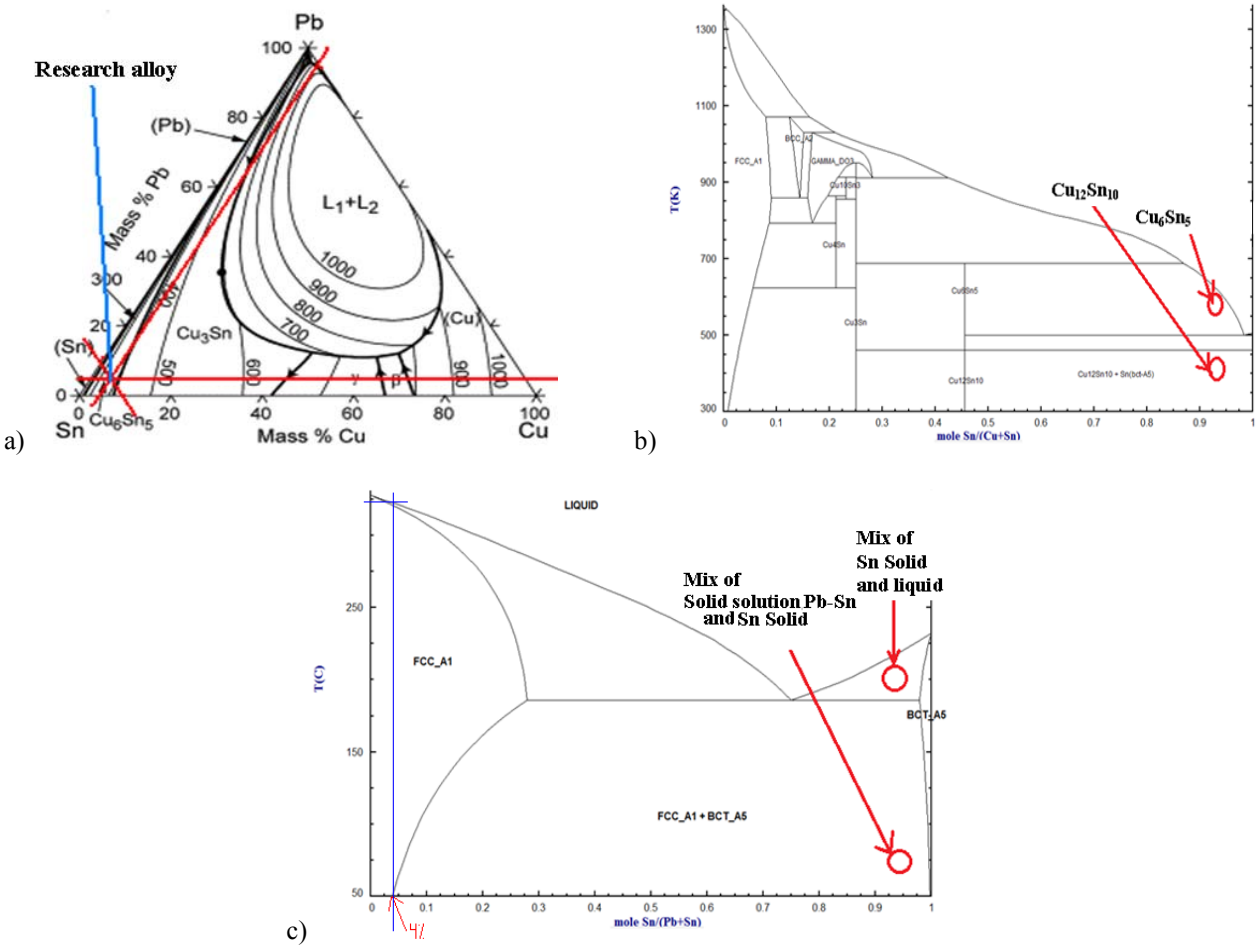

Fig. 1.a) Ternary phase diagram Sn-Cu-Pb[8], b) Binary phase diagram Sn-Cu[9], c) Binary phase diagram Sn-Pb[9],[10]

2. Experimental methods

According Figure 2 (b), in the horizontal centrifugal casting to do not fall down the molten from highest part of mold, the centrifugal force must be greater than or equal to the force of gravity. It means that the equation 1 must be established.

$$F = m \times r \times \omega^2 \geq m \times g \rightarrow r \times \omega^2 \geq g \rightarrow \frac{r \times \omega^2}{g} \geq 1$$

$$\rightarrow \omega^2 \geq \frac{g}{r} \rightarrow \omega \geq \sqrt{\frac{g}{r}} \rightarrow \omega \geq \sqrt{\frac{g}{(R-t)}} \qquad (1)$$

g is 9.8 m/sec2, r is inner radius (free surface) of product in meter, R is outer radius of product (or inner radius of mold) in meter, t is thickness of product in meter and ω is rotation speed of mold in rotation per seconds for production of sound cast with thickness of t.

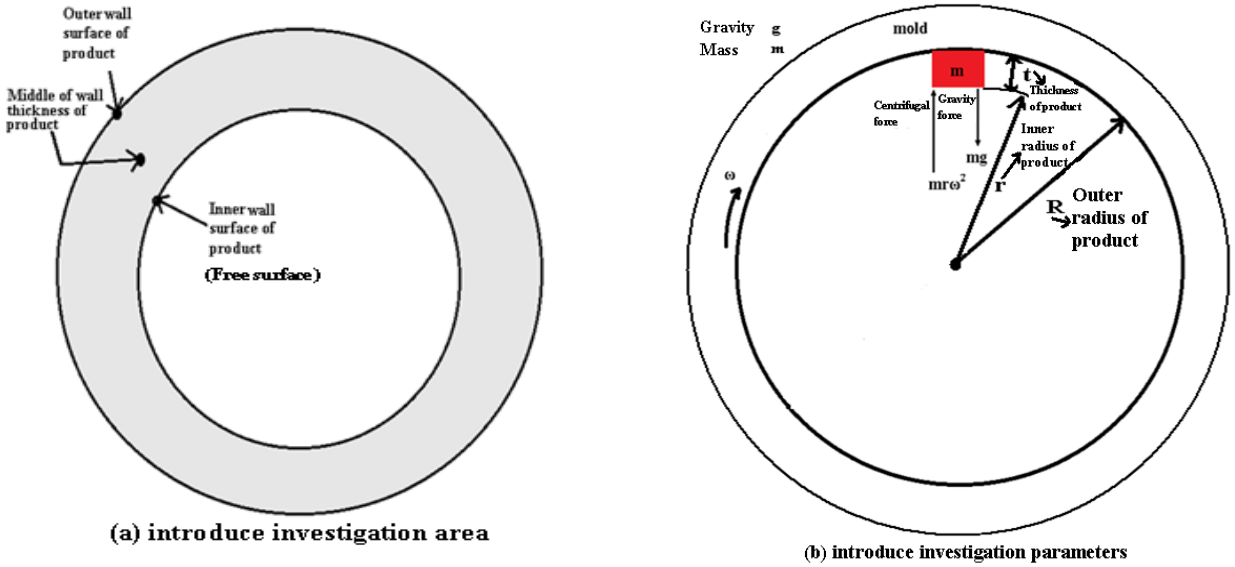

Fig. 2. The horizontal centrifugal casting

In Figure 3, the components of a centrifugal casting machine were shown. DC Electro motor 0.55 kW of DUTCHI NL along with converter of TECO E310 series 200V class were used to varying rotation speed of the mold.Hot work tool steel AISI H11 mold with thickness of 6 and the length of 240, diameter of 200 mm (L/D ratio equal to 1.2) and a mold slope of 2 % was used. To prevent sticking of the product, the inner surface of the mold will be covered with slurry of sand (with a thin thickness).

According to equation 1, to produce a sound cast, the minimum required rotation speed of mold is calculated equal to 594 rpm. According to equation 1, as the product thickness is increased, the rotation speed of mold should be increased to produce a sound cast. For example, to produce a product with thickness of 12 mm, the mold rotation speed must be increased to 633 rpm.

$$t = 0 \qquad \rightarrow \omega_{t=0cm} = \sqrt{\frac{g}{r = (R - t)}} = \frac{980\ \frac{cm}{sec^2}}{10\ cm} \cong 9.9\ \frac{1}{sec} = 594\ rpm$$

$$t = 1.2 \qquad \rightarrow \omega_{t=1.2cm} = \sqrt{\frac{g}{r = (R - t)}} = \frac{980\ \frac{cm}{sec^2}}{8.8\ cm} \cong 10.55\ \frac{1}{sec} = 633\ rpm$$

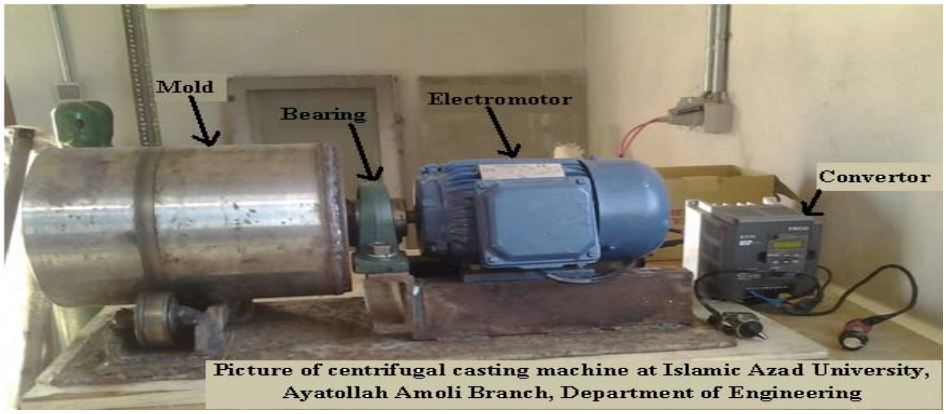

Fig. 3. Components of a centrifugal casting machine

At first, 480 grams of commercial pure copper ingots was melted in the crucible furnace with diesel fuel. After adding 11700 grams commercial pure tin ingots and completely melting it, 390 grams commercial pure lead ingots were added and thoroughly stirred. Thus, the alloy containing 92.7% tin, 3.8% copper and 3.1% lead were produced and poured in horizontal centrifugal casting machine and a product was made in the shape of a hollow cylinder with a length of 24 cm, an external diameter of 20 cm

and a thickness of 12 mm. Molten was runner into the cold mold (not preheated) with debi of 2178.22 g/(cm2.sec), molten pouring time set to 5 sec, a pouring temperature of 390 ° C and a runner height of 43 cm. Mold rotation speed at first was 600 rpm that is increased to 640 rpm until the end of melting process. After finishing work, a product with thickness 10 mm was obtained.

3. Results and discussion

The total chemical composition of the Babbitt alloy (an alloy of tin base) in this study were determined according to JIS H 1141 reference standard of in Razi Metallurgical Research Center and listed in Table 1.

Table 1.
Total chemical composition of SnCu4Pb3Wt%

Al	Sb	Bi	Cd	Cu	Zn	Pb	Ag	Sn	Fe
0.01<	0.01<	0.02	0.02	3.8	0.1	3.1	0.005	92.7	0.02

Hardness testing was performed according to ASTM E384-11 [11] standard reference with Vickers method using an indentation diamond pyramid with a force of 300 gram force in Razi Metallurgical Research Center. Hardness testing results in three regions (Fig. 2 (a)) were listed in Table 2. The maximum bulk hardness is in the outer surface of the product.

Table 2.
Bulk hardness, grain size, distance of solid solution Pb-Sn particles, content and distance of intermetallic Cu_6Sn_5 particles

Distance from free surface	Average bulk hardness	Average amount of intermetallic Cu_6Sn_5 particle	Average distance from intermetallic Cu_6Sn_5 particle	Average distance from Pb-Sn solid solution particle	Average grain size
0 mm	17.7 HV	Zero	There is no particle	80.5 μm	100 μm
5 mm	14 HV	0.84 Vol%	70 μm	76.4 μm	70 μm
10 mm	14.7 HV	1.23 Vol%	50 μm	73.2 μm	50 μm

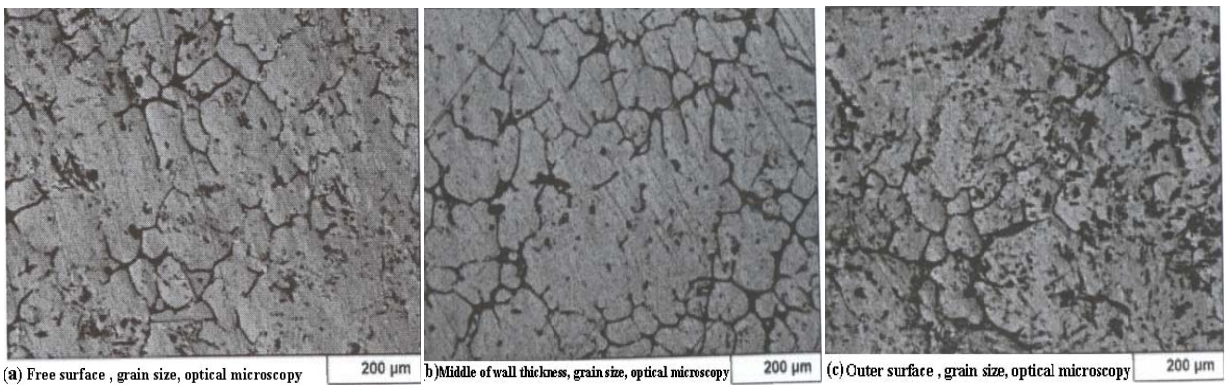

Fig. 4. Optical microscope, etching solution Nital 2%

Metallographic sample was prepared according to ASTM E3-11 [12] standard and etch of samples were selected according to ASTM E407-07 [13] standard. A 2% Nital was used as etch solution to reveal the structure of tin-copper intermetallic compound, lead-tin solid solution phase and to image microstructure granularity. Optical microscope (OM) images were prepared according to the standard of ASTM E883-11 [14] in Razi Metallurgical Research Center

Granularity image of the outer surface with a size of 50 microns and a free surface with a size of 100 microns and the middle of thickness of product with a grain size of 70 microns is shown in Figure 4.

In Table 2, the grain size has been decreased from the inner (free) surface to the outer surface of the product. Because mold that was made of metal was not preheated and so cooling speed of molten was decreased with distance from the surface of metal mold. Thus, an area that is closer to the metal mold has been cooled faster and so it is fine, and an area that is far from the mold has been cooled more slowly and therefore it is coarser

Overall, the bulk hardness should be increased with fine grains [15], but the results in Table 2 do not show this fact. Because the grain size at the free surface of the product (100 μm) is greater than the grain size in the middle of thickness of product (70 μm) and the hardness of the free surface of the product (14.7 HV) is larger than in the middle of thickness of the product (14 HV). Thus, other factors such as hard phases are dominant compared to the grain size. Above matter is validated by attention to the higher amount of hard intermetallic particles (Cu_6Sn_5) in the outer surface of the product (Table 2 and Fig. 5b) compared to middle of thickness of the product (Table 2 and Fig. 5c).

Average distance of solid solution of lead-tin (white continuous phase) from each other in the three areas, including the free surface of the product (an average distance of 80.5 μm), middle of thickness of product (an average distance of 76.4 μm according to Figure 5 (a)) and the outer surface of the product (an average distance of 73.2 μm) were calculated and are listed in Table 2

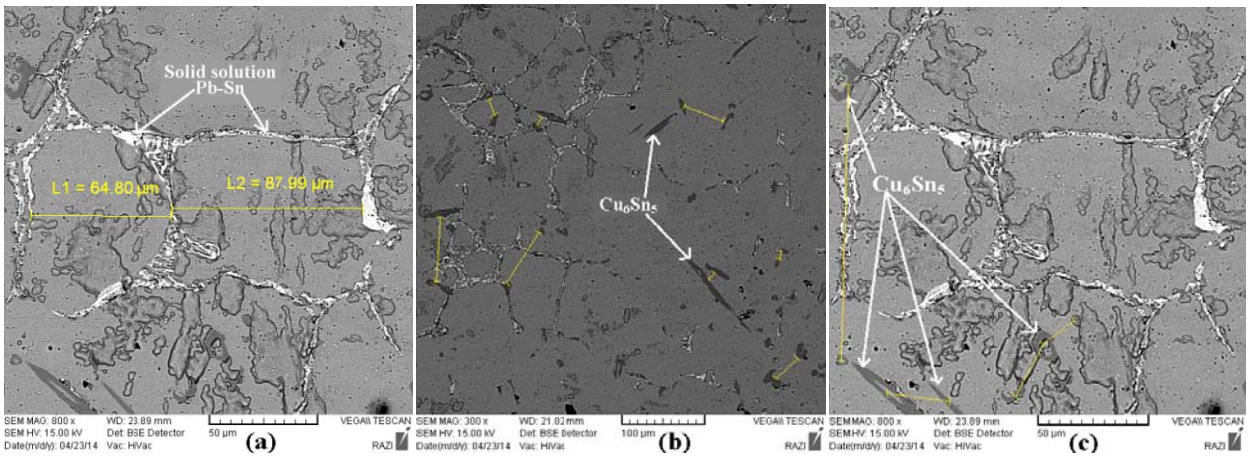

Fig. 5. SEM images (a) Average distance of solid solution of lead-tin (white continuous phase) from each other in the middle of thickness of product (b) Average distance of Cu_6Sn_5 (dark gray needle shaped phase) particles in the outer surface of the product, (c) Average distance of Cu_6Sn_5 particles in the middle of thickness of the product

In Figure 5a can be observed that a large amount of solid solution of lead-tin (continuous white phase) is located at the grain boundaries. Due to the relative heaviness of the solid solution of lead (92.85 wt %) and tin (7.15 wt %) compared to other phases (consisting of tin matrix and copper-tin intermetallic particles), compaction of solid solution of lead - tin has declined as away from the product of mold.

Distances between phases of copper-tin intrametallic compound (dark gray needle shaped phase) in a tin matrix in three areas including, the free surface of the product (particles were not observed), middle of thickness of product (an average distance of 70 microns as shown in Figure 5 (b)) and the outer surface of the product (an average distance of 50 micron as shown in Figure 5 (c)) were calculated and are listed in Table 2.

Due to the intermetallic compound particles are lighter than the molten phase and the solid solution, therefore it is expected to increase intermetallic compound particles with distance from the mold wall. Whereas, observations in Figure 5 (b), Figure 5 (c) and Table 2 clearly show that the amount of intermetallic particles near the wall of mold (outer surface of product, 1.23 Vol%) is more than other areas such as the middle of the thickness of the product (0.84 Vol%) because the critical velocity of the interface movement (or solidification velocity in not preheated mold) is more than intermetallic particles movement velocity for moving from the outer surface of the product to the free surface of the product. For this reason, the particles in the back of interface of solidification are pressed. In the other words, the solidification front prevents from moving of the intermetallic particles to the free surface of the product. So that intermetallic particles are not observed on the free surface of the product (farthest point to the mold wall).

Variable amounts of hardness and Cu_6Sn_5; grain size and phase distance from each other versus the distance from the free surface of the product that is given in Table 2 is plotted in Figure 6 for easier comparison.

By comparing the variable changes with the distance from the free surface of the product in Figure 6, it can be inferred that high hardness (17.7 HV) in the outer surface of the product is related to simultaneous effect of fine grain size (50 µm) in this area and large amount of hard intermetallic particles (with an average content of 1.23 Vol%).

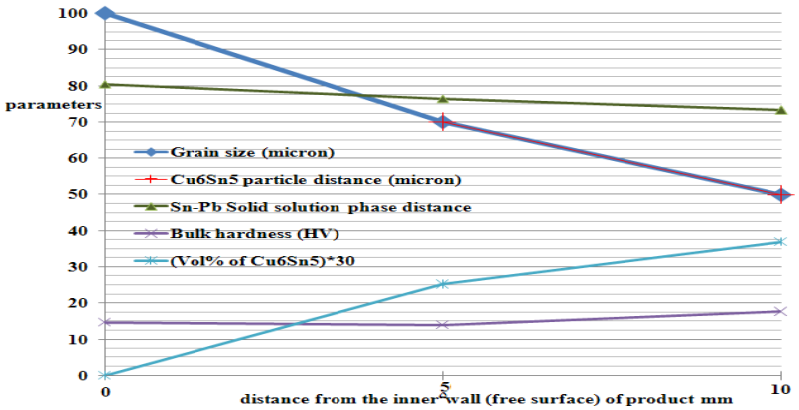

Fig. 6. Variables amounts of hardness and Cu_6Sn_5; grain size and phase distance from each other versus the distance from the free surface of the product

Exact determination of chemical composition of the intrermetallic particles and the solid solution phase was performed from the spectrum of energy dispersive (Energy Dispersive Spectroscopy, EDS) using a scanning electron microscope of TESCAN VEGA II (SEM) in the mentioned areas in Figure 2 (a), in Razi Metallurgical Research Center. Quantitative and qualitative amount of elements in solid solution Pb - Sn were observed and shown in Figure 7. In addition, the quantitative and qualitative amounts of elements in the intermetallic compound (Cu_6Sn_5) were observed and were shown in Figure 8.

As shown in Figure 7, the solid solution of 92.85 wt% Pb and 7.15 wt% Sn were identified. These values are in a good accordance with the theoretical values of 2.39 wt % tin and 97.61 wt% Pb. This solid solution (phase A) is shown in the SEM as a bright white phase

As shown in Figure 8, intermetallic compound Cu_6Sn_5 is detected as 40.37 atomic percent tin and 59.63 atomic percent copper. These values are in a good accordance with the theoretical values of 5/11×100=45.45% atomic percent tin and 6/11×100=54.55% atomic percent copper. This intermetallic compound (phase B) is shown in the SEM as a dark gray phase

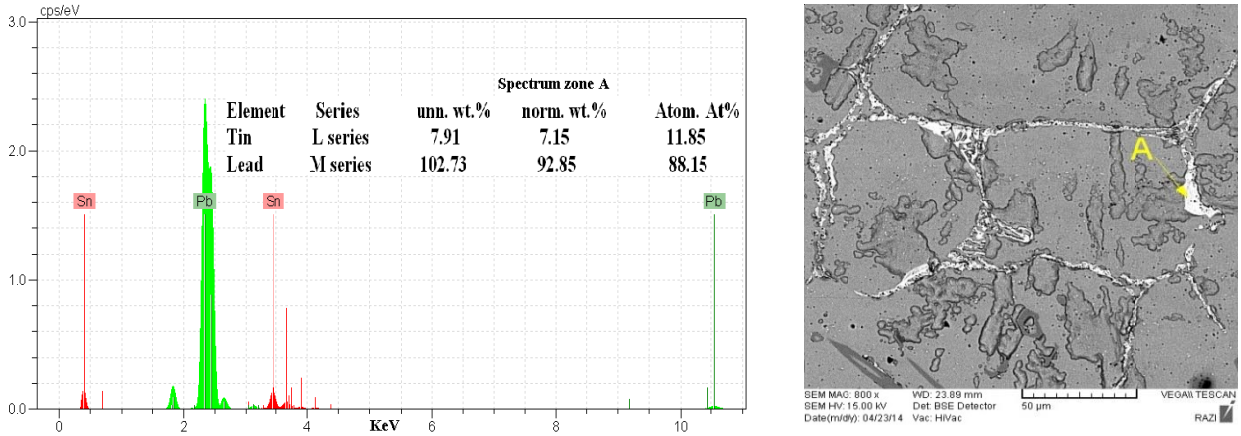

Fig. 7. SEM with EDS of solid solution Pb-Sn (phase of A), Back scattered Electron (BSE), magnification of 800

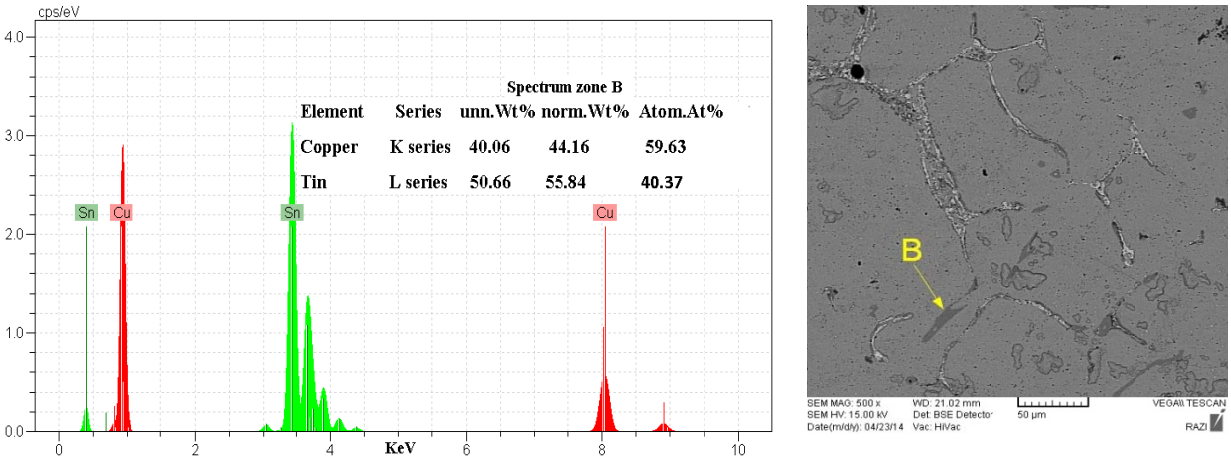

Fig. 8. SEM with EDS of intermatallic Cu_6Sn_5 particles (phase of B), Back scattered Electron (BSE), magnification of 500

4. Conclusions

In this study, hardness and microstructure of the functionally graded product in the shape of a hollow cylinder with a length of 24 cm and an external diameter of 20 cm and a thickness of 12 mm, made from SnCu4Pb3 which was made by the horizontal centrifugal casting method were studied in three regions. Consequently, to achieve desired hardness (17.7 HV) in a specific area of product must be pointed tointeraction of two microstructure factors including grain size (50 µm) and the amount of hard intermetallic Sn_5Cu_6 particles (1.23 Vol%).

Acknowledgement

The financial assistance received from the University Grants Commission, Department of Engineering- Ayatollah Amoli Branch- Islamic Azad University- Amol- Iran to carry out a part of this research is gratefully acknowledged.

References

[1] Jorstad, J.L. (2008). Centrifugal Casting. In: Marquard, E. Lampman, H. editors. *ASM Handbook Volume 15*: Casting. Ohio, USA: ASM International, Materials Park;. 665-84.

[2] Kapranos, P. Carney, C. Pola, A Jolly, M. (2014). 5.03 - Advanced Casting Methodologies: Investment Casting, Centrifugal Casting, Squeeze Casting, Metal Spinning, and Batch Casting. In: Hashmi, S. Batalha, GF. Tyne, CJV. Yilbas, B. editors. *Comprehensive Materials Processing*. Oxford: Elsevier; 39-67.

[3] Lin, X. Liu, C. Xiao, H. (2013). Fabrication of Al–Si–Mg functionally graded materials tube reinforced with in situ Si/Mg2Si particles by centrifugal casting. *Composites Part B: Engineering.45*. 8-21.

[4] Luo, D. Wang, H-Y. Ou-Yang, Z-T. Chen, L. Wang, J-G.Jiang, Q-C. (2014). Microstructure and mechanical properties of Mg–5Sn alloy fabricated by a centrifugal casting method. *Materials Letters116*. 108-11.

[5] Rahvard, M.M. Tamizifar, M. Boutorabi, S.M.A. Gholami Shiri, S. (2014). Characterization of the graded distribution of primary particles and wear behavior in the A390 alloy ring with various Mg contents fabricated by centrifugal casting. *Materials & Design56*. 105-14.

[6] Vadayar, K.S. Rani, SD. (2014). Characterization of Sn-Bi and Sn-Bi-Zn alloys.*Advanced Materials Manufacturing and Characterization4*51-6.

[7] Cullity, B.D. (1978). *Elements of X-ray Diffraction*. Second ed. London, England: Addison-Wesley publishing company, Inc.

[8] Kong, L-X. Yang, B. Xu, B-Q.Li, Y-F. Li, L. Liu, D-C, et al. (2013). Application of molecular interaction volume model in separation of Pb–Sn–Sb ternary alloy by vacuum distillation. *Transactions of Nonferrous Metals Society of China23*. 2408-15.

[9] Smith, J.F. (2007). Chapter one - Introduction to phase diagrams. In: Zhao, JC, editor. *Methods for Phase Diagram Determination*. Oxford: Elsevier Science Ltd;. 1-21.

[10] Massalski, T.B. (2001). Phase Diagrams. In: Buschow KHJ, Cahn RW, Flemings MC, Ilschner B, Kramer EJ, Mahajan S, et al., editors. Encyclopedia of Materials: Science and Technology (Second Edition). Oxford: Elsevier. 6842-51.

[11] A.S.T.M. E384-11, Standard Test Method for Knoop and Vickers Hardness of Materials. Ohio, USA: ASM international; 2011.

[12] A.S.T.M. E3-11, Standard Guide for Preparation of Metallographic Specimens. Ohio, USA: ASM international; 2011.

[13] A.S.T.M. E407-07, Standard Practice for Microetching Metals and Alloys. Ohio, USA: ASM international; 2007.

[14] A.S.T.M. E883-11, Standard Guide for Reflected–Light Photomicrography. Ohio, USA: ASM international; 2011.

[15] Dieter, GE. (2000). Mechanical Behavior under tensile and compressive loads. In: Kuhn, H. Medlin, D. editors. Mechanical Testing and Evaluation. Ohio: ASM international5, 100-3.